Revue des Composites et des Matériaux Avancés-Journal of Composite and Advanced Materials
Vol. 35, No. 1, February, 2025, pp. 43-49
Journal homepage: http://iieta.org/journals/rcma

Physicochemical Characteristics of PCL-Chi/Mwcnt/AgNPS Nanofibers for the Adsorption of Glyphosate Herbicide in Water

J. N. Salgado-Delgado[1], N. K. R. Bogireddy[2], A. M. Salgado-Delgado[1], R. Salgado-Delgado[1], U. León-Silva[3], R. E. Nuñez-Gomez[1], A. Olarte-Paredes[1]*

[1] División de Estudios Profesionales de Posgrado e Investigación, Tecnológico Nacional de México/IT de Zacatepec, Zacatepec 62780, Mexico
[2] Biofísica y Ciencia de Materiales, Instituo de Ciencias Físicas, Universidad Nacional Autónoma de México, Cuernavaca 62209, México
[3] Centro de In Centro de Investigación en Ingeniería y Ciencias Aplicadas, Universidad Autónoma del Estado de Morelos, Cuernavaca 62209, México

Corresponding Author Email: alfredo.op@zacatepec.tecnm.mx

https://doi.org/10.18280/rcma.350106

Received: 16 December 2024
Revised: 14 January 2025
Accepted: 16 February 2025
Available online: 28 February 2025

Keywords:
glyphosate, green synthesis, electrospinning, herbicide adsorption, silver nanoparticles, polycaprolactone

ABSTRACT

The study presents a novel approach by developing biodegradable nanofibers from polycaprolactone (PCL) and chitosan (Chi) by electrospinning to address the excessive use of herbicides. Multi-walled carbon nanotubes (MWCNT) and silver nanoparticles (AgNPs) were incorporated to enhance the adsorption of glyphosate (Gly). AgNPs were previously synthesized by a green method using the extracts of Porophyllum ruderale (P. Ruderale) and Pithecellobium dulce (P. dulce). FTIR spectroscopy characterized the nanofibers, revealing specific functional groups of PCL, at 1728 cm^{-1} and 1153 cm^{-1} the carbonyl C=O and carboxyl stretching respectively. Mechanical tests, contact angle measurements and morphological analysis by SEM showed that the addition of Chi increased the strength of the material from 74 MPa to 79 MPa, the hydrophobicity decreased from 105º to 90º and by SEM it was observed that the nanofibers were more uniform having a thickness size between 100 nm and 200 nm. The diffractogram corresponding to PCL-Chi presented two characteristic peaks of biopolymers, the main one at 2θ=23.13º and a second peak at 2θ=13.58º, indicating that the material has a semicrystalline structure. The adsorption of the nanofibers to Gly was studied with the UV-Vis spectroscopy technique, by linear regression the final concentrations of Gly were obtained, finding that Chi and AgNPs play an important role in the absorption due to the electrostatic interactions between Gly. UV-Vis analysis showed the highest adsorption capacity in sample PCL-Chi/1:2G100 0.1 with 0.262g Gly/g of membrane due to the stability and surface area of AgNPs. This unique material, with its herbicide adsorption potential, offers a new perspective for addressing soil and water pollution and associated health problems.

1. INTRODUCTION

Herbicides are chemicals that control and eliminate undesirable plants such as grasses and shrubs. One of the negatie points of using herbicides is that weeds can become resistant to the products, and also cause water and soil contamination. Among the most widely used pesticides is the herbicide Glyphosate (Gly), N-(phosphonomethyl) glycine ($C_3H_8NO_5P$), it is use was expanded under the assumption that side effects were minimal [1]. However, growing concerns have arisen about the direct and indirect impacts of Gly on the health [2]. In 2015, the WHO published a report considering Gly as 'probably carcinogenic to humans,' causing pathologies such as liver and kidney damage, tumor formation, cancer, spontaneous abortions, and disruptions to the endocrine system [3].

Rainio et al. [4] researched the effects of Gly-based herbicides on detoxification pathways among invertebrates. They conducted two different types of experiments: one was a direct treatment with pure Gly and Gly-based herbicides, and the second was an indirect treatment only with Gly-based herbicides in food, evaluated in the beetle insect because it has the greatest metabolic resistance. Demonstrating that pure Gly increased the probability of higher mortality but in the indirect experiment they did not conclude that it may be due to the short evaluation time.

Gly is a non-selective synthetic herbicide, it is colorless and odorless, and it is highly soluble in water, contains an amino glycine group, which produces zwitterions, that is, a molecule that has a dipole moment between the phosphonic and carboxylic acid and the protonated amino group [5]. Currently, the methods for the remediation and detection of Gly are

expensive, in addition to producing secondary contaminants that make it difficult to eliminate this herbicide [6].

Do et al. [7] studied the optical method based on Surface Plasmon Resonance with a Chi membrane and nanocomposites such as zinc oxide (ZnO) and graphene oxide (GO) as a biosensor for the detection of Gly using the spin-coating technique. Their results showed that a thin film with ZnO has a higher sensitivity for the detection of Gly, they evaluated the selectivity for Gly metabolite molecules such as AMPA and glufosinate, where they showed that it has good selectivity for Gly but not for the other molecules, which does not yet occur in aqueous systems.

In the current research, PCL-Chi/MWCNT/AgNPs nanofibers were fabricated using the electrospinning method, a novel technique for producing nanofibers with high porosity and large surface area [8]. Diel et al. [9] functionalized multiwalled carbon nanotubes with iron nanoparticles through green synthesis to eliminate Gly. They studied the adsorption percentages of Gly using isotherms, reaching 86.23% and equilibrium after 2 h, being promising for the treatment of water with Gly.

Rozo et al. [10] investigated, silicon nanopillars and a silver layer to detect and adsorb Gly and AMPA using Surface Enhanced Raman Spectroscopy. The studies carried out revealed that there are chemical interactions, confirming it with the density functional theory that the main interaction is with the oxygen of the carboxylic acid and phosphate and for AMPA it is with the nitrogen of the amino.

PCL is a biodegradable synthetic polymer that is non-toxic and has good mechanical properties [11]. It exhibits high thermal stability compared to other aliphatic polyesters; however, it has high hydrophobicity, limiting Gly adsorption [12]. Therefore, Chi was added to modify its structure by the presence of amino ($-NH_2$) and hydroxyl (-OH) groups, imparting hydrophilicity to PCL [13]. Additionally, nanomaterials such as MWCNT and AgNPs were added to increase adsorption capacity, mechanical resistance, high surface area, and chemical stability [8, 13, 14], thus generating a promising biomaterial for Gly adsorption in contaminated water, which can attract Gly through electrostatic forces [15].

2. MATERIALS AND METHODS

2.1 Materials

Polycaprolactone (ALDRICH, CAS: 24980-41-4), 2,2,2-Trifluoroethanol (ALDRICH, CAS: 75-89-8), Chitosan (ALDRICH, CAS: 9012-76-4, average molecular weight), Multi-walled carbon nanotubes (ALDRICH, CAS: 308068-56-6, >90% carbon basis, DxL 110-170 nmx5.9μm), Acetic acid (ALDRICH, CAS: 64-19-7), Silver Nitrate (Analytical reagent, A.C.S. 5g, CAS: 7761-88-8), Ethanol (Merck, CAS: 64-17-5), Glyphosate (New Cap, Aqueous solution).

2.2 Experimental design

Table 1 presents the 2k (k=2) experimental design, with 2 factors (MWCNT and AgNPs) and 2 levels in each factor (0.1% and 0.3%). A comprehensive collection process yielded fourteen samples, each with their respective replicas. PCL (polycaprolactone)-Chi (chitosan) are placed for the sample key. Finally, the nanomaterials are added: MWCNT (multi-walled carbon nanotubes) and AgNPs (silver nanoparticles), and the percentage added of each nanomaterial to each sample (0.1% and 0.3%). That percentage was used to observe the influence between the quantity of the materials, in addition, lower the quantity of nanomaterials improve the properties such as material resistance, chemical stability, surface area, and adsorption of contaminants such as herbicides [16].

2.3 Methodology

A 10% PCL solution was prepared, dissolving PCL in 2,2,2-trifluoroethanol (TFE) and homogenizing it with an ultrasonic bath (BRANSON). Chi was prepared at 3% (w/v) in a solution of acetic acid/distilled water at 2% (v/v) by homogenizing through the sonication process [8]. The same thorough homogenization process was used to combine Chi and PCL solutions.

2.4 Fabrication of green synthesis mediated AgNPs

For the green synthesis of AgNPs, we exercised strict control over the process. Extracts of P. Ruderale and P. Dulce were obtained by mixing 20g of plant leaves with an 80% ethanol solution as a solvent, macerating with a mortar and pestle. The extract was obtained by heating the macerated mixture to 90°C and 100°C. When reaching these temperatures, a 0.1M $AgNO_3$ solution was slowly added, dropping. The temperature was meticulously controlled and the solution constantly stirred to avoid AgNPs fluctuations. The solution turns dark brown, indicating the formation of AgNPs [17], then it is cooled to room temperature (25°C).

MWCNT and AgNPs were added to the polymeric matrix according to Table 1, using the ultrasonic bath to disperse them in the solution for 3 h.

Table 1. Nanofiber working matrix

Sample	PCL/Chi (v/v)	MWCNT (%)	AgNPs (%)
PCL	10/0	0	0
PCL-Chi	4/1	0	0
PCL-Chi/MWCNT 0.1	4/1	0.1	0
PCL-Chi/MWCNT 0.3	4/1	0.3	0
PCL-Chi/1:2G90 0.1	4/1	0	0.1
PCL-Chi/1:2G90 0.3	4/1	0	0.3
PCL-Chi/1:2G100 0.1	4/1	0	0.1
PCL-Chi/1:2G100 0.3	4/1	0	0.3
PCL-Chi/1:3P90 0.1	4/1	0	0.1
PCL-Chi/1:3P90 0.3	4/1	0	0.3
PCL-Chi/1:3P100 0.1	4/1	0	0.1
PCL-Chi/1:3P100 0.3	4/1	0	0.3

2.5 Nanofibers

The electrospinning equipment, a Model CRT40X2199 Spellman High Voltage DC Supply, connected to a voltage source with a rotating aluminum roller collector and a grounding connector, was used for nanofiber production. The

solution was deposited in a syringe with a gravity flow applying a voltage of 22kV, and the distance from the needle tip to the collector was 15cm [18]. The syringe was carefully set to rotate at 200rpm for an exposure time of 6 hours, ensuring precise control over the process. Waxed paper covered the collector roller and gathered the nanofibers [19].

2.6 Glyphosate adsorption

The Gly calibration curve was obtained using the UV-Vis spectrophotometer equipment Velab, and it was evaluated in Gly solutions with concentrations from 0.1M to 0.5M. The maximum absorption at 220nm was recorded for each solution [20].

2.7 Nanofiber characterization

Fourier Transform Infrared Spectroscopy (FTIR) performed nanofiber characterization to observe the characteristic functional groups of the nanofibers, using the Perkin Elmer Spectrum Two ATR equipment in the spectral range between 4000-500cm^{-1} (Chalfont Rd, Seer Green, Beaconsfield HP9 2FX, UK). Morphological analysis was carried out by Scanning Electron Microscopy (SEM) JEOL brand (JSM 6010A, Musashino, Akishima, Tokyo 196-8558, Japan) in SEI mode and 1.5 kV with metallic coating. The mechanical tests, conducted with the utmost thoroughness, were evaluated on the INSTRON universal machine, model Instron 3340, according to ASTM D-882 standard, with a standard film tension at a speed of 0.5 m/s. The contact angle was measured with a 1µL goniometer with distilled water on the membrane surface at room temperature (25°C), and photos of the micro drop were taken with a 3s exposure on the membrane.

3. RESULTS

3.1 Morphological study

Figure 1(A) presents the histograms and micrographs at 10,000x magnification of Figure 1 (A1) PCL and Figure 1 (B) PCL-Chi. In Figure 1 (A2), we observed tiny droplets of the solution in the electrospinning process, with their diameter increasing, possibly due to the viscosity of PCL [21, 22] or the electric field generated between the solution and the collector roller. This led to varied sizes in histogram, with an approximate average of 150nm. However, in Figure 1 (A3), we noticed a significant change. Chi, a key component, contributed to a remarkable improvement in uniformity, as droplets like those in Figure 1(A4) were no longer visible. The histogram showed an average size of around 100nm. Energy Dispersive Spectroscopy (EDS) analysis was conducted to quantify the elements present. It demonstrated that the MWCNT samples contained 70% carbon and 30% oxygen [16].

In the micrographs of Figure 1 (A5)-(A6), a secondary network of fibers was observed, likely due to the increased conductivity generated by Chi and AgNPs, causing the fibers to break into smaller sizes [23]. Additionally, the AgNPs were dispersed very sparsely on the surface of the nanofibers, likely due to the low concentration applied. The nanofibers had an average size of 90-500nm [24]. Similarly, in the EDS analysis, Ag was observed dispersed within the nanofibers, constituting 100% of the composition.

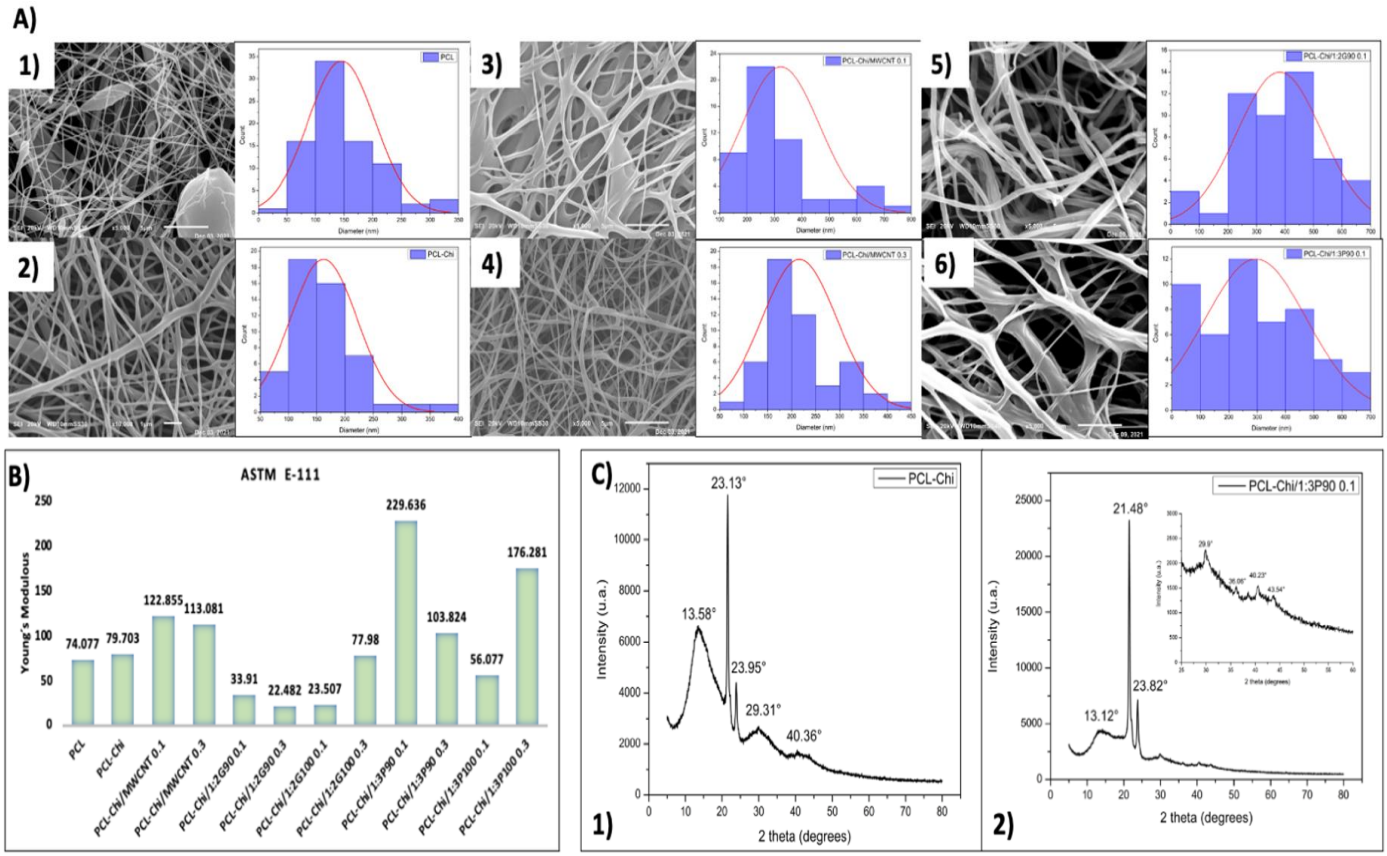

Figure 1. A) Histograms and micrographs of 1) PCL, 2) PCL-Chi, 3) PCL-Chi/MWCNT 0.1, 4) PCL-Chi/MWCNT 0.3, 5) PCL-Chi/1:3P90 0.1, 6) PCL-Chi/1:3P90 0.3. B) Young´s modulus (Mpa). C) X-ray diffraction (XRD) 1) PCL-Chi, 2) PCL-Chi/1:3P90 0.1

3.2 Mechanical tests

The analysis of mechanical tensile tests was conducted according to the ASTM E-111 standard, a standard method for Young's modulus, tangent modulus, and chord modulus. A comparison was made with the results obtained in the mechanical analysis using the Instron universal machine. The tests were conducted at a speed of 0.55 m/s, and to facilitate the test, the nanofibers were cut into dimensions of 20 mm width by 60 mm length, and the thickness of each sample was measured [13].

Table 2 and Figure 1 (B) present the results of Young's modulus (ε). The PCL sample exhibited ε=74.077MPa due to surface roughness and the formation of droplets caused by increased viscosity, as observed in Figure 1 (A1) and (A2). However, upon adding Chi to the PCL material, its strength increased slightly, with ε=79.703MPa. This increase in strength can be attributed to the electrostatic forces between PCL and Chi and the uniformity in fiber size [13], which prevents clustering between the materials.

Table 2. Results of Young´s modulus (MPa)

Sample	ASTM E-111	Standard Deviation
PCL	74.077	0.291
PCL-Chi	79.703	0.914
PCL-Chi/MWCNT 0.1	122.855	0.465
PCL-Chi/MWCNT 0.3	113.081	0.965
PCL-Chi/1:2G90 0.1	33.910	0.001
PCL-Chi/1:2G90 0.3	22.482	0.124
PCL-Chi/1:2G100 0.1	23.507	0.085
PCL-Chi/1:2G100 0.3	77.980	0.435
PCL-Chi/1:3P90 0.1	229.636	1.493
PCL-Chi/1:3P90 0.3	103.824	1.123
PCL-Chi/1:3P100 0.1	56.077	0.453
PCL-Chi/1:3P100 0.3	176.281	0.681

The distribution between the nanomaterials and the polymer matrix is well-maintained, with no observed clustering, and their viscosity does not lead to an increase in fiber size. As the percentage of nanomaterial addition decreases, the material's strength increases [17]. The material that stands out with the highest strength is PCL-Chi/1:3P90 0.1, boasting an impressive 229.636MPa. The addition of small quantities of AgNPs further enhances particle-matrix stability [16-18]. The key to this enhancement lies in the better dispersion of AgNPs in the fibers, facilitated by van der Waals forces. This improved dispersion leads to a more excellent resistance [18], as the AgNPs tend to deform less, resulting in good interaction.

3.3 Structural analysis using X-Ray diffraction

Figure 1 (C) illustrates the X-ray diffraction (XRD) patterns of PCL and Chi. In Figure 1 (C1), the characteristic peak at 13.58°, which corresponds to Chi in the anhydrous form C-O-C, indicates the presence of both crystalline and amorphous parts in Chi. This finding, as Sánchez et al. [25] noted in 2016, underscores the excellent stability of the biopolymer structure. Peaks at 23.13° and 23.95° correspond to PCL, suggesting that the nanofibers possess a semicrystalline structure [7].

In Figure 1 (C2), PCL-Chi/1:3P90 0.1. The characteristic signal of the PCL-Chi structure decreases, suggesting that the AgNPs improve the material distribution, establishing a more coherent relationship between the polymeric matrix and the reinforcement. Slight curves are observed at angles 29°, 40°, and 43°, attributed to the AgNPs [26], corresponding to the planes of the silver-centered cubic structure. Though of lower intensity, these curves are due to the lower content of AgNPs compared to the matrix.

3.4 Functional groups study by FTIR

Figure 2 (A) shows the FTIR spectrum of PCL and PCL-Chi samples in the wavelength range of 4000-500cm^{-1}. In 2948 and 2860cm^{-1}, the asymmetric and symmetric CH_2 stretching is shown, at 1728cm^{-1}, the carbonyl C=O stretching (characteristic functional group of PCL), and at 1153cm^{-1}, the C-O stretching present in the Chi structure [21]. No changes in functional groups were observed, attributing to the absence of chemical bonding between PCL and Chi in the membrane. Additionally, it may be due to the higher concentration of PCL [11].

3.5 Hydrophobic analysis

Figure 2 (B) shows the contact angle results of the nanofibers. The PCL sample exhibited 110° hydrophobic characters due to the presence of ester groups like the carbonyl group C=O, limiting its application in Gly adsorption. Therefore, Chi was added to PCL, conferring hydrophilicity with 95° due to hydroxyl and amino groups. The use of nanomaterials such as MWCNT and AgNPs influences the contact angle. It was observed that the material's hydrophobicity increased with a lower percentage of addition [26].

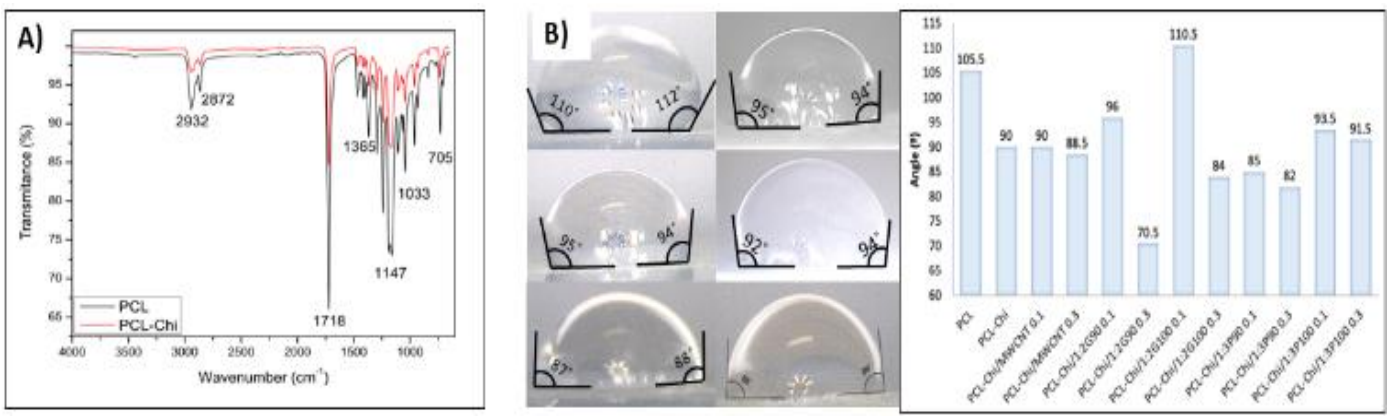

Figure 2. A) FTIR spectrum of PCL and PCL-Chi, B) Contact angle

3.6 Glyphosate adsorption

Figure 3 shows the reaction mechanism of PCL-Chi/Gly, the adsorption of Gly is generated by hydrogen bonds between the hydroxyl and amino groups of Gly and Chi.

Figure 4 (A1) to Figure 4 (A3) present the FTIR spectra of Gly PCL/Gly and PCL-Chi/Gly. Notably, signals were detected at 3335cm^{-1} corresponding to the stretching of the hydroxyl group -OH, at 1606cm^{-1} indicating NH bending, at 1207 representing the P-OH group, at 1110cm^{-1} for P-O, at 808cm^{-1} for P-C, all unique characteristic groups of Gly, and at 730cm^{-1} for the out-of-plane -OH bending.

Adsorption analysis was performed by UV-Vis Spectroscopy. Figure 4 (B1) shows the spectrum of Gly, a maximum adsorption was observed at the wavelength of 220nm. The adsorption analysis was evaluated in a time of 30 min, with the linear equation obtained from the regression the final concentration of Gly adsorbed on the membrane is evaluated (Figure 4 (B2)).

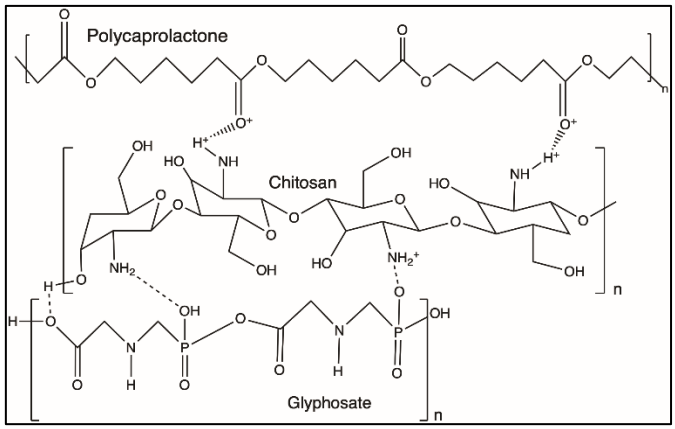

Figure 3. Mechanism of possible reaction among PCL-Chi/Gly

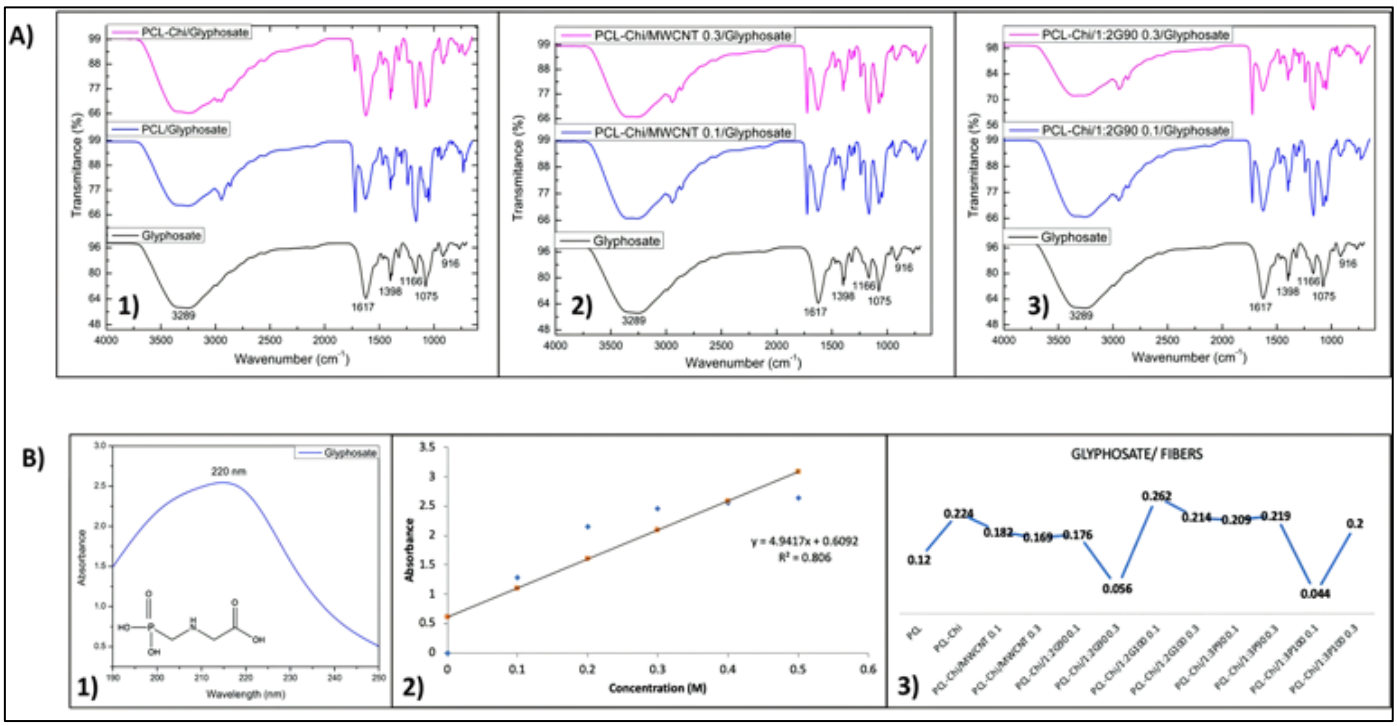

Figure 4. A) FTIR spectra of 1) Glyphosate and PCL, 2) B) Glyphosate adsorption

Table 3 and Figure 4(B3) present the results of Gly adsorption by the membrane sample. It was observed that the addition of Chi to PCL significantly enhances the adsorption of Gly. The sample that exhibited the best adsorption effectiveness was PCL-Chi/1:2G100 0.1, adsorbing 0.262g of Gly per gram of membrane. The morphological analysis showed homogeneity in the fibers, as well as an average diameter of 90-100 cm and a good dispersion of the AgNPs, giving stability to the surface for the adsorption of Gly. It is observed that AgNPs reinforce the matrix and have the property of stabilizing the environment in which they are found, Gly can have various adsorption mechanisms, one of them is by the secondary amine that it has in its molecular structure because it has the ability to generate hydrogen bonds or van der Waals forces, on the other hand, Chi is essential and can be adsorbed by charges, remembering that it has a strong positive charge and Gly is negative, it also has hydroxyl groups where they can generate hydrogen bonds [2]. Additionally, it achieved an angle of 98º, ideal for Gly adsorption, as it is not highly hydrophobic, and part of the material has a hydrophilic character [27].

Table 3. Glyphosate adsorption

Sample	% Adsorption	g Gly/g Membrane
PCL	7.10	0.12
PCL-Chi	13.25	0.22
PCL-Chi/MWCNT 0.1	10.80	0.18
PCL-Chi/MWCNT 0.3	12.51	0.16
PCL-Chi/1:2G90 0.1	13.01	0.17
PCL-Chi/1:2G90 0.3	3.31	0.05
PCL-Chi/1:2G100 0.1	15.50	0.26
PCL-Chi/1:2G100 0.3	12.66	0.21
PCL-Chi/1:3P90 0.1	12.40	0.20
PCL-Chi/1:3P90 0.3	13.00	0.21
PCL-Chi/1:3P100 0.1	2.60	0.04
PCL-Chi/1:3P100 0.3	11.83	0.20

Our process revealed that adding Gly to the PCL sample results in the appearance of the carbonyl signal characteristic of the PCL structure. This signal decreases when Chi is added, indicating a breaking of carbonyl bonds. The signals are influenced during adsorption, and the phosphate groups are modified in the 1050 cm^{-1} signal, possibly due to the stabilization of radicals. This careful study underscores the role of hydroxyl groups in forming hydrogen bonds with Gly [1-28].

4. CONCLUSION

In this study, we successfully fabricated PCL-Chi/MWCNT/AgNPs nanofibers, demonstrating novel properties for Gly adsorption in water pollution, which were evaluated under laboratory conditions. Gly, with its net negative charge due to the phosphates in its molecule, interacts with the nanofibers containing Chi and AgNPs, which possess a positive charge. This unique electrostatic and intermolecular interaction enables effective Gly adsorption. The sample that demonstrated the best adsorption effectiveness was PCL-Chi/1:2G100 0.1, adsorbing 0.262g of Gly per gram of membrane. The addition of Chi to the material decreased its hydrophobicity, enhancing adsorption properties. The hydrophilic part of Chi facilitated the interaction of hydroxyl groups to bind the contaminant, as shown in FTIR. The functional groups in adsorption are phosphates and carbonyl C=O, facilitating interaction between Gly molecules and nanofibers. These findings demonstrate the potential of the obtained material for Gly adsorption, providing a solid foundation for future research in this area, to observe the reduction of this negative implication of Gly in rivers and oceans.

REFERENCES

[1] Zúñiga, K., Rebollar, G., Avelar, M., Campos-Terán, J., Torres, E. (2022). Nanomaterial-based sensors for the detection of glyphosate. Water, 14(15): 2436. https://doi.org/10.3390/w14152436

[2] Lach, P., Garcia-Cruz, A., Canfarotta, F., Groves, A., Kalecki, J., Korol, D., Borowicz, P., Nikiforow, K., Cieplak, M., Kutner, W., Piletsky, S.A., Sharma, P.S. (2023). Electroactive molecularly imprinted polymer nanoparticles for selective glyphosate determination. Biosensors and Bioelectronics, 236: 115381. https://doi.org/10.1016/j.bios.2023.115381

[3] Gonzales Molfino, H.M., Alcalde Yañez, A., Valverde Morón, V.V., Villanueva Salvatierra, D.V. (2020). Electrospinning: Advances and applications in the field of biomedicine. Revista de La Facultad de Medicina Humana, 20(4): 706-713. https://doi.org/10.25176/rfmh.v20i4.3004

[4] Rainio, M.J., Margus, A., Tikka, S., Helander, M., Lindström, L. (2023). The effects of short-term glyphosate-based herbicide exposure on insect gene expression profiles. Journal of Insect Physiology, 146: 104503. https://doi.org/10.1016/j.jinsphys.2023.104503

[5] Sen, K., Mondal, N.K. (2021). Statistical optimization of glyphosate adsorption by silver nanoparticles loaded activated carbon: Kinetics, isotherms and thermodynamics. Environmental Nanotechnology, Monitoring and Management, 16: 100547. https://doi.org/10.1016/j.enmm.2021.100547

[6] Zambotti, A., Bruni, A., Biesuz, M., Sorarù, G.D., Rivoira, L., Castiglioni, M., Onida, B., Bruzzoniti, M.C. (2023). Glyphosate adsorption performances of polymer-derived SiC/C aerogels. Journal of Environmental Chemical Engineering, 11(3): 109771. https://doi.org/10.1016/j.jece.2023.109771

[7] Do, M.H., Dubreuil, B., Peydecastaing, J., Vaca-Medina, G., Nhu-Trang, T.T., Jaffrezic-Renault, N., Behra, P. (2020). Chitosan-based nanocomposites for glyphosate detection using surface plasmon resonance sensor. Sensors (Switzerland), 20(20): 1-19. https://doi.org/10.3390/s20205942

[8] Olarte-Paredes, A., Salgado-Delgado, J.N., Rubio-Rosas, E., Salgado-Delgado, A.M., Hernández-Cocoletzi, H., Salgado-Delgado, R., Moreno-Carpintero, E., Castaño, V.M. (2021). Physico-Chemical properties of a hybrid biomaterial (Pva/chitosan) reinforced with conductive fillers. Applied Sciences (Switzerland), 11(7): 3040. https://doi.org/10.3390/app11073040

[9] Diel, J.C., Franco, D.S.P., Nunes, I.D.S., Pereira, H.A., Moreira, K.S., Thiago, T.A., Foletto, E.L., Dotto, G.L. (2021). Carbon nanotubes impregnated with metallic nanoparticles and their application as an adsorbent for the glyphosate removal in an aqueous matrix. Journal of Environmental Chemical Engineering, 9(2): 105178. https://doi.org/10.1016/j.jece.2021.105178

[10] Rozo, C., Wu, K., Rindzevicius, T., Boisen, A., Castillo, J.J. (2021). Surface-enhanced raman spectroscopy and density functional theory study of glyphosate and aminomethylphosphonic acid using silver capped silicon nanopillars. Universitas Scientiarum, 26(1): 51-67. https://doi.org/10.11144/Javeriana.SC26-1.srsa

[11] Sadeghi, A., Mousavi, S.M., Saljoughi, E., Kiani, S. (2021). Biodegradable membrane based on polycaprolactone/polybutylene succinate: Characterization and performance evaluation in wastewater treatment. Journal of Applied Polymer Science, 138(18): 1-14. https://doi.org/10.1002/app.50332

[12] Rafiei, M., Jooybar, E., Abdekhodaie, M.J., Alvi, M. (2020). Construction of 3D fibrous PCL scaffolds by coaxial electrospinning for protein delivery. Materials Science and Engineering C, 113: 110913. https://doi.org/10.1016/j.msec.2020.110913

[13] Doan, H.N., Vo, P.P., Baggio, A., Negoro, M., Kinashi, K., Fuse, Y., Sakai, W., Tsutsumi, N. (2021). Environmentally friendly chitosan-modified polycaprolactone nanofiber/nanonet membrane for controllable oil/water separation. ACS Applied Polymer Materials, 3(8): 3891-3901. https://doi.org/10.1021/acsapm.1c00463

[14] Encinas Basurto, D.A., Alvarez Carvajal, F., Armenta Calderon, A., Gonzalez Soto, T.E., Esquer Miranda, E., Juarez Onofre, J., Mendez Ibarra, R. (2020). Silver nanoparticles coated with chitosan against Fusarium oxysporum causing the tomato wilt. Biotecnia, 22(3): 73-80. https://doi.org/10.18633/biotecnia.v22i3.952

[15] Zhao, Y.X., Chen, Q.M., Zhang, C., Li, C.N., Jiang, Z.L., Liang, A.H. (2022). Aptamer trimode biosensor for trace glyphosate based on FeMOF catalytic oxidation of tetramethylbenzidine. Biosensors, 12(11): 920. https://doi.org/10.3390/bios12110920

[16] Kumar, A., Sharma, K., Dixit, A.R. (2021). A review on the mechanical properties of polymer composites reinforced by carbon nanotubes and graphene. Carbon Letters, 31: 149-165. https://doi.org/10.1007/s42823-020-00161-x

[17] Salgado-Delgado, J.N., Salgado-Delgado, A.M., Salgado-Delgado, R., Granados-Baeza, M.J., Rubio-Rosas, E., Olarte-Paredes, A. (2023). Optimization with 2K factorial design in green synthesis of silver nanoparticles (AgNPs) using Porophyllum ruderale extract. Journal of Applied Research and Technology, 21(6): 1042-1049. https://doi.org/10.22201/icat.24486736e.2023.21.6.2042

[18] Herrero-Herrero, M., Alberdi-Torres, S., González-Fernández, M.L., Vilariño-Feltrer, G., Rodríguez-Hernández, J.C., Vallés-Lluch, A., Villar-Suárez, V. (2021). Influence of chemistry and fiber diameter of electrospun PLA, PCL and their blend membranes, intended as cell supports, on their biological behavior. Polymer Testing, 103: 107364. https://doi.org/10.1016/j.polymertesting.2021.107364

[19] Park, H., May, A., Portilla, L., Dietrich, H., Münch, F., Rejek, T., Sarcletti, M., Banspach, L., Zahn, D., Halik, M. (2020). Magnetite nanoparticles as efficient materials for removal of glyphosate from water. Nature Sustainability, 3(2): 129-135. https://doi.org/10.1038/s41893-019-0452-6

[20] O'Connor, R.A., Cahill, P.A., McGuinness, G.B. (2021). Effect of electrospinning parameters on the mechanical and morphological characteristics of small diameter PCL tissue engineered blood vessel scaffolds having distinct micro and nano fibre populations - A DOE approach. Polymer Testing, 96: 107119. https://doi.org/10.1016/j.polymertesting.2021.107119

[21] Mohamady Hussein, M.A., Guler, E., Rayaman, E., Cam, M.E., Sahin, A., Grinholc, M., Sezgin Mansuroglu, D., Sahin, Y.M., Gunduz, O., Muhammed, M., El-Sherbiny, I.M., Megahed, M. (2021). Dual-drug delivery of Ag-chitosan nanoparticles and phenytoin via core-shell PVA/PCL electrospun nanofibers. Carbohydrate Polymers, 270: 118373. https://doi.org/10.1016/j.carbpol.2021.118373

[22] Fahimirad, S., Abtahi, H., Satei, P., Ghaznavi-Rad, E., Moslehi, M., Ganji, A. (2021). Wound healing performance of PCL/chitosan based electrospun nanofiber electrosprayed with curcumin loaded chitosan nanoparticles. Carbohydrate Polymers, 259: 117640. https://doi.org/10.1016/j.carbpol.2021.117640

[23] Mojarad Shafiee, B., Torkaman, R., Mahmoudi, M., Emadi, R., Derakhshan, M., Karamian, E., Tavangarian, F. (2020). Surface modification of 316L SS implants by applying bioglass/gelatin/polycaprolactone composite coatings for biomedical applications. Coatings, 10(12): 1220. https://doi.org/10.3390/coatings10121220

[24] Pattanashetti, N.A., Achari, D.D., Torvi, A.I., Doddamani, R.V., Kariduraganavar, M.Y. (2020). Development of multilayered nanofibrous scaffolds with PCL and PVA: NaAlg using electrospinning technique for bone tissue regeneration. Materialia, 12: 100826. https://doi.org/10.1016/j.mtla.2020.100826

[25] Sánchez Cepeda, Á.P. (2016). Preparation and characterization of electrospun polymeric membranes of polycaprolactone and chitosan for controlled release of thiamine chlorhydrate. Ciencia en Desarrollo, 7(2): 133-152. https://doi.org/10.19053/01217488.v7.n2.2016.4818

[26] Mirda, E., Idroes, R., Khairan, K., Tallei, T.E. et al. (2021). Synthesis of chitosan-silver nanoparticle composite spheres and their antimicrobial activities. Polymers, 13(22): 3990. https://doi.org/10.3390/polym13223990

[27] Ortiz, L.A., Ramiro, E., Rao, F. (2022). El ángulo de contacto y su relación con las propiedades superficiales en un sistema orgánico-líquido-gas. Journal of Chemical Engineering Theoretical and Applied Chemistry, 79(595): 224-230. https://raco.cat/index.php/afinidad/article/view/397432.

[28] Diyanat, M., Saeidian, H., Baziar, S., Mirjafary, Z. (2019). Preparation and characterization of polycaprolactone nanocapsules containing pretilachlor as a herbicide nanocarrier. Environmental Science and Pollution Research, 26(21): 21579-21588. https://doi.org/10.1007/s11356-019-05257-0

NOMENCLATURE

AMPA	Aminomethylphosphonic acid
AP	Precursor agent
AR	Reductor agent
ASTM	American Society for Testing and Materials
ANOVA	Analysis of variance
°C	Centigrade
XRD	X-ray diffraction
FTIR	Fourier Transform Infrared Spectroscopy
K	Factor
GO	Graphene
Gly	Glyphosate
g	Grams
h	Hours
kV	Kilovolts
W	Wavelength
MPa	Megapascals
m	Meters
mL	Milliliters
SEM	Scanning Electron Microscopy
ε	Elasticity modulus
M	Molar
nm	Nanometers
AgNPs	Silver nanoparticles
$XAgNO_3$	Silver nitrate
WHO	World Health Organization
ZnO	Zinc Oxide
PCL	Polycaprolactone
P. Ruderale	Porophyllum Ruderale
P. Dulce	Pithecellobium Dulce
Chi	Chitosan
SPR	Surface plasmon resonance
s	Seconds
v	Volume
TFE	2,2,2-Trifluoroethanol